

## A PILOT SEARCH FOR EVIDENCE OF EXTRASOLAR EARTH-ANALOG PLATE TECTONICS

M. JURA<sup>1</sup>, B. KLEIN<sup>1</sup>, S. XU (许偲艺)<sup>1</sup>, AND E. D. YOUNG<sup>2</sup>

<sup>1</sup> Department of Physics and Astronomy, University of California, Los Angeles, CA 90095-1562, USA;

[jura@astro.ucla.edu](mailto:jura@astro.ucla.edu), [kleinb@astro.ucla.edu](mailto:kleinb@astro.ucla.edu), [sxu@astro.ucla.edu](mailto:sxu@astro.ucla.edu)

<sup>2</sup> Department of Earth, Planetary, and Space Sciences, University of California,  
Los Angeles, CA 90095, USA; [eyoung@ess.ucla.edu](mailto:eyoung@ess.ucla.edu)

Received 2014 June 20; accepted 2014 July 18; published 2014 August 6

### ABSTRACT

Relative to calcium, both strontium and barium are markedly enriched in Earth’s continental crust compared to the basaltic crusts of other differentiated rocky bodies within the solar system. Here, we both re-examine available archived Keck spectra to place upper bounds on  $n(\text{Ba})/n(\text{Ca})$  and revisit published results for  $n(\text{Sr})/n(\text{Ca})$  in two white dwarfs that have accreted rocky planetesimals. We find that at most only a small fraction of the pollution is from crustal material that has experienced the distinctive elemental enhancements induced by Earth-analog plate tectonics. In view of the intense theoretical interest in the physical structure of extrasolar rocky planets, this search should be extended to additional targets.

*Key words:* planetary systems – planets and satellites: composition – stars: abundances – white dwarfs

*Online-only material:* color figures

### 1. INTRODUCTION

Internal melting and the subsequent differentiation into an iron-dominated core, a magnesium-elevated mantle and a silicon-rich crust are central to the evolution of the solar system’s rocky planets. Located on the surface, crusts are the most easily studied of these three different zones, and, when examined in detail, they display a wide variety of elemental compositions (Taylor & McLennan 2009). While other crusts are largely basaltic, Earth’s continental crust is compositionally unique (Rudnick & Gao 2003) because, as a consequence of plate tectonics, it is the product of the partial melting of preexisting oceanic crustal material—itsself basaltic—that results in striking enrichments in “incompatible” elements by magmatic distillation.

The possibility that extrasolar rocky planets undergo plate tectonics has been extensively discussed (Valencia et al. 2007; O’Neill & Lenardic 2007; Valencia & O’Connell 2009; Kite et al. 2009; Korenaga 2010; Stamenkovic et al. 2011, 2012; van Heck & Tackley 2011; van Summeren et al. 2011; Foley et al. 2012; O’Rourke & Korenaga 2012; Stein et al. 2013; Bercovici & Yanick 2013). Much of this effort has been motivated by the recognition that plate tectonics may affect a planet’s habitability (Korenaga 2012). However, current observational tests of whether extrasolar rocky planets experience plate tectonics have seemed unrealistic (Lenardic & Crowley 2012). Here, we argue that an indirect search for the operation of Earth-analog plate tectonics on extrasolar rocky planets is possible because of the unique chemical signature that would be produced in the spectrum of an externally polluted white dwarf.

The generally accepted standard model for the presence of elements heavier than helium in the atmospheres of white dwarfs cooler than 20,000 K is that these stars have accreted tidally disrupted asteroids (Debes & Sigurdsson 2002; Jura 2003; Jura & Young 2014). As a zero-order approximation, it has been found that as with bulk Earth, major constituents of extrasolar planetesimals are oxygen, magnesium, silicon, and iron (Zuckerman et al. 2007; Klein et al. 2010, 2011;

Gaensicke et al. 2012; Jura et al. 2012; Xu et al. 2013, 2014). No truly exotic objects as predicted by Bond et al. (2010)—such as being carbon-/silicon-dominated or calcium-/aluminum-/oxygen-dominated—have been found (Jura & Xu 2012). Consequently, it seems that geophysical models for the origin and evolution of rocky objects developed for the solar system may be extended to extrasolar planetesimals.

Evidence is now strong that extrasolar planetesimals have experienced igneous differentiation (Jura et al. 2013; Jura & Young 2014) with individual accreted parent bodies understood as measurably consisting of an Fe-rich core (Gaensicke et al. 2012), an Fe-poor mantle (Farihi et al. 2013), an Al-rich crust (Zuckerman et al. 2011), or a mixture of core and crustal material (Xu et al. 2013). Internal heating and the subsequent melting from the decay of <sup>26</sup>Al can plausibly help explain these results (Jura et al. 2013).

Fragments of evolved planetesimals or even entire planets may be separated from their parent body by collisions and subsequently accrete onto the white dwarf while retaining their distinctive compositional signature. Here, we assess whether there is even a modest contribution from continental crust-analog material to the total accretion onto two well observed white dwarfs. That is, although the bulk of matter accreted onto white dwarfs originates in asteroids, there inevitably must be some collisional erosion of the surface of a rocky planet which would result in some planetary crustal material also contributing to the pollution of the host star. In the solar system, there is an exchange among the terrestrial planets of impact ejecta (Gladman et al. 1996; Treiman et al. 2000); similar processes must occur in extrasolar environments.

In Section 2, we first describe what we might expect for extrasolar basaltic and continental crustal compositions by extrapolating from the solar system. Because Sr and Ba overabundances relative to Ca are uniquely high in Earth’s continental crust, we then assess available evidence for the concentrations of these two elements in two externally polluted white dwarfs in Section 3. Finally, in Section 4, we discuss our results and summarize our conclusions.

**Table 1**  
Crustal Abundance Ratios by Mass Relative to Ca

Crust	Mg	Fe	Sr	Ba	Reference
Earth—continental	0.62	1.1	7.0e-3	0.010	(1)
Earth—oceanic	0.62	0.89	1.1e-3	7.3e-5	(2)
Lunar highland	0.24	0.31	1.2e-3	6.1e-4	(3)
Mars	1.1	2.8	7.1e-4	1.1e-3	(3), (4)
Vesta	0.58	2.0	1.0e-3	2.3e-4	(5)
CI meteorites	11	20	8.6e-4	2.5e-4	(6)

**References.** (1) Rudnick & Gao 2003; (2) N-MORB [= Normal Mid-Ocean Ridge Basalt] from Taylor & McLennan 2009; (3) Taylor & McLennan 2009; (4) Sr from Shergotty meteorite (McSween 1985); (5) Sioux County Eucrite (Mittlefehldt 2004); (6) Wasson & Kallemeyn 1988.

## 2. CRUSTAL ELEMENTAL COMPOSITIONS: SOLAR SYSTEM

Although there are many imaginable routes for the formation and evolution of extrasolar rocky planets, we develop our expectations of extrasolar crustal compositions from those four solar system bodies for which detailed abundance measurements of their crusts have been achieved: Earth, the Moon, Mars, and Vesta (Taylor & McLennan 2009). In all cases, the two most abundant elements are O and Si, with enhanced concentrations of Al and Ca. Because they are largely sequestered into the core and mantle, respectively, Fe and Mg are deficient.

Compared to basaltic crusts, Earth’s continental crust is compositionally unique: “incompatible” elements are highly concentrated within this outermost zone containing about 0.6% of the planet’s mass (Rudnick & Gao 2003). Lying in the same column of the periodic table, Ca, Sr, and Ba—three incompatible elements of interest here—have relatively large ionic radii that are accommodated by the more silica- and Al-rich tectosilicates that form from the crystallization of the partial melts of oceanic plate material. The consequent coalescence of the products of melting in the form of island arcs (for example, Japan) produces continental crust that persists because it is too buoyant to be subducted. The most pronounced chemical enrichment occurs for Ba, the largest atom.

We list in Table 1 the mass concentrations relative to Ca of selected key elements in the four best-studied solar system crusts. In the crusts of the Moon, Mars, and Vesta, Sr and Ba are at most modestly enhanced relative to Ca, while both elements are markedly enhanced in Earth’s continental crust and modestly depleted in Earth’s oceanic crust. Therefore, simultaneous substantial enhancements of  $n(\text{Sr})/n(\text{Ca})$  and  $n(\text{Ba})/n(\text{Ca})$  can serve as an observational signature of Earth-analog plate tectonics.

For reference, we also list in Table 1 the abundances in CI chondrites, the assumed approximate initial nebular composition before the rocky objects formed and evolved. Reddy et al. (2003) reported abundances of 27 elements in a sample of 181 nearby F- and G-type main sequence stars spanning a wide range of ages. The Ca, Sr, and Ba abundances are almost always within 0.10 dex of the solar value. Therefore, the approximation that planets form from an extrasolar nebular with a solar composition is appropriate. Furthermore, because the condensation temperatures of Ca, Sr, and Ba are very similar (Lodders 2003), we expect that separation of these elements occurs in post-nebular physical processing. The most familiar cosmochemical pathway for a dramatic enhancement of the strontium and barium abundances occurs during plate tectonics.

## 3. STRONTIUM AND BARIUM MEASUREMENTS: EXTRASOLAR PLANETESIMALS

To date, no purely crustal material has been detected in an externally polluted white dwarf (Jura & Young 2014). That is, while there is good evidence for differentiation, there is no star where Si and O are the dominant pollutants. Instead, observed accreted material is composed of blends of core, mantle, and crust. Here, we picture that while most of the accretion onto externally polluted white dwarfs derives from asteroids, there may be collisional erosion of the crust of a planet and this debris could contribute to the total inflow.

### 3.1. Model

Consider now the standard model to estimate the elemental composition of the parent body (or bodies) from measurements of photospheric abundances. The mass of the  $Z$ ’th element in the outer mixing zone of a white dwarf,  $M_*(Z)$ , is governed by the rate of mass gain from accretion from a parent body (or parent bodies),  $\dot{M}_{\text{PB(S)}}(Z)$ , and the rate of mass loss described by settling with the expression (Koester 2009)

$$\frac{dM_*(Z)}{dt} = -\frac{M_*(Z)}{t_Z} + \dot{M}_{\text{PB(S)}}(Z), \quad (1)$$

where  $t_Z$  denotes the  $Z$ ’th element’s settling time. We spectroscopically determine  $M_*(Z)$  in the star’s outer mixing zone.

Here, we picture that  $\dot{M}_{\text{PB(S)}}(Z)$  is dominated by the contribution from asteroids,  $\dot{M}_{\text{Ast}}(Z)$  but there may be an additional contribution from a continental crust,  $\dot{M}_{\text{CC}}(Z)$ . Therefore,

$$\dot{M}_{\text{PB(S)}}(Z) = \dot{M}_{\text{Ast}}(Z) + \dot{M}_{\text{CC}}(Z). \quad (2)$$

One solution to Equation (1) is that the system is in a steady state and the accretion is ongoing. In this case, if  $\dot{M}_{\text{PB(S)}}(Z)$  is constant, the approximate solution is that

$$M_*(Z) \approx \dot{M}_{\text{PB(S)}}(Z) t_Z. \quad (3)$$

If so, then for any two elements denoted by  $j$  and  $k$ , the ratio between the masses of detectable material in the parent body (or bodies) is

$$\frac{\dot{M}_{\text{PB(S)}}(Z_j)}{\dot{M}_{\text{PB(S)}}(Z_k)} = \frac{M_*(Z_j) t_{Z,k}}{M_*(Z_k) t_{Z,j}}. \quad (4)$$

In this case, in order to determine the abundances, the relative settling times must be computed in addition to measuring the relative photospheric abundances.

While many different histories can be imagined, the simplest and most straightforward is that the accretion from both the asteroids and planetary crusts is in a steady state and that Equation (4) pertains. Consider now a simple two-source model where both asteroids with a composition similar to CI chondrites and continental crust material contribute to the accretion. Define  $f_{\text{CC}}$ , the proportion of continental crust material, as

$$f_{\text{CC}} = \frac{\dot{M}_{\text{CC}}(\text{Ca})}{\dot{M}_{\text{Ast}}(\text{Ca})}. \quad (5)$$

Using the relative abundances in Table 1, we can use Equations (2) and (5) to write that

$$\dot{M}_{\text{PB(S)}}(\text{Ca}) = \dot{M}_{\text{Ast}}(\text{Ca})(1 + f_{\text{CC}}), \quad (6)$$

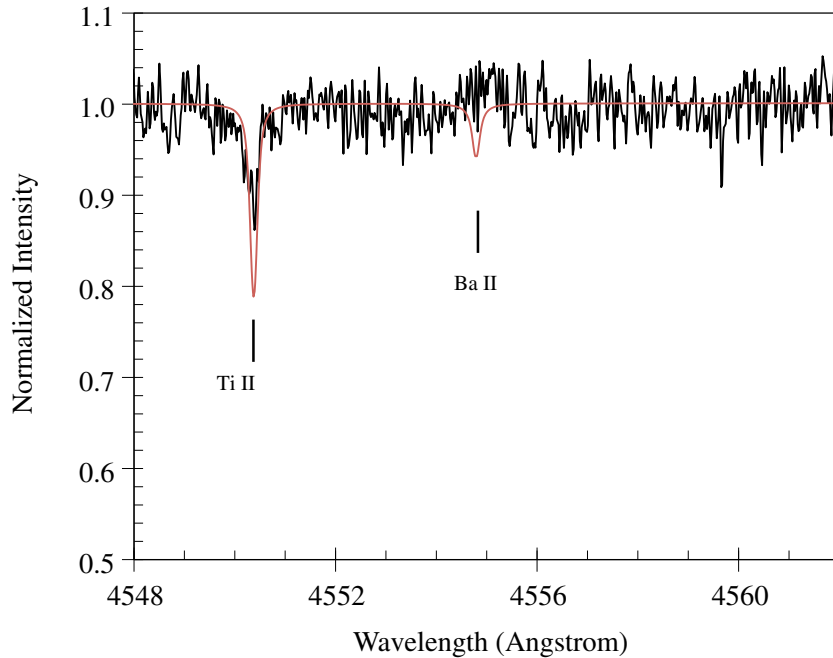


**Figure 1.** Spectrum of GD 362 in the vicinity of Ba II 4554 Å. Black denotes the data while red denotes the model with our inferred upper limit to the Ba abundance given in Table 2. The model is wavelength-shifted to the photospheric frame of the star; the equivalent width of Ba II 4554 Å is 18 mÅ. Wavelengths are in the air and the heliocentric frame of rest.

(A color version of this figure is available in the online journal.)

and

$$\dot{M}_{\text{PB(S)}}(\text{Ba}) = 2.5 \times 10^{-4} \dot{M}_{\text{Ast}}(\text{Ca})(1 + 40 f_{\text{CC}}). \quad (7)$$

We combine Equations (6) and (7) to find

$$\frac{(1 + 40 f_{\text{CC}})}{(1 + f_{\text{CC}})} = \left( \frac{\dot{M}_{\text{PB(S)}}(\text{Ba})}{\dot{M}_{\text{PB(S)}}(\text{Ca})} \right) (2.5 \times 10^{-4})^{-1}. \quad (8)$$

From measurements of the calcium and barium accretion rates, we use Equation (8) to solve for  $f_{\text{CC}}$ .

### 3.2. Targets

Here, we consider two of the best studied externally polluted white dwarfs: GD 362 (Zuckerman et al. 2007; Xu et al. 2013) and PG 1225–079 (Klein et al. 2011; Xu et al. 2013), where it is already known that the relative abundances are non-chondritic. Both stars have exceptionally strong Ca II 3933 Å and Ca II 3968 Å with a blended equivalent width larger than 15 Å. Because Ca, Sr, and Ba all lie in the same column of the periodic table, their ground state resonance lines all lie on approximately the same curve of growth in the spectra of white dwarfs, and we can measure Sr and Ba abundances near  $10^{-4}$  that of Ca to make useful comparisons with the ratios listed in Table 1. On the basis of its having marked excess infrared emission with a prominent  $10 \mu\text{m}$  emission feature, GD 362 is modeled to have a dust disk with an inner temperature greater than 1000 K (Becklin et al. 2005; Kilic et al. 2005; Jura et al. 2007) and therefore is likely mostly accreting from a single asteroid (Jura 2008). Although PG 1225–079 does have a modest infrared excess at  $8 \mu\text{m}$  (Farihi et al. 2010), the inferred maximum dust temperature is only about 300 K. There is likely a large inner hole in the disk, and there may be significant contributions to the accretion from more than one parent body (Farihi et al. 2010; Xu et al. 2013).

We use the same theoretical model atmospheres computed by D. Koester as employed in Xu et al. (2013) and described in Koester (2010). We have also adopted the stellar effective temperatures and gravities given in Xu et al. (2013). The atomic parameters for Ba are taken from Mashonkina et al. (1999). The settling times, as based on the formalism of Koester (2009) and subsequently updated,<sup>3</sup> for Ca, Sr, and Ba are computed to equal  $9.6 \times 10^4$  yr,  $4.7 \times 10^4$  yr, and  $3.9 \times 10^4$  yr, respectively, for GD 362. For PG 1225–079, the updated settling times for Ca, Sr, and Ba are  $1.9 \times 10^6$  yr,  $1.4 \times 10^6$  yr, and  $1.0 \times 10^6$  yr, respectively.<sup>4</sup> The ratios of the settling times used in Equation (4) are more confidently known than their absolute values (Xu et al. 2013) which are not required for this analysis.

At the factor of two level, the chemistry of Ca in extrasolar planetesimals is uncertain (Jura & Young 2014). Here, we focus on enhancements of between a factor of 10 and 100 which are much greater than the current observational or geochemical uncertainties.

### 3.3. Barium Limits

Barium has not been detected nor does it have quantitative upper limits to its abundance previously been reported in any externally polluted white dwarf. Therefore, we have re-examined archived Keck/HIRES spectra to place upper limits to the Ba abundance from Ba II 4554 Å, as illustrated in Figures 1 and 2. Using the same model atmosphere analysis as in Xu et al. (2013), we report in Table 2 our derived upper limits both to the Ba abundances and our estimates of the mass accretion rates of Ba and Ca from Equation (4). The previously measured Ca

<sup>3</sup> Timescales can be taken from <http://www.astrophysik.uni-kiel.de/~koester/astrophysics/> and further discussed in Xu et al. (2013).

<sup>4</sup> There is a typographical error in Table 5 of Xu et al. (2013); the units for the settling time should have been given as  $10^6$  yr.

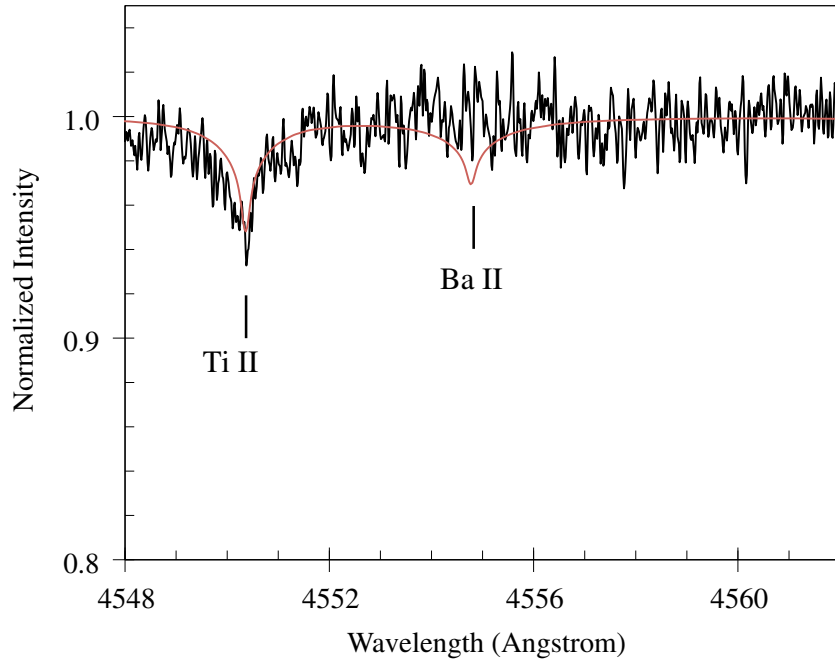


**Figure 2.** Same as Figure 1, except for the spectrum of PG 1225–079. Here, the equivalent width of the model Ba II 4554 Å line is 35 mÅ. (A color version of this figure is available in the online journal.)

**Table 2**  
Results for Ca, Sr, and Ba

Star	$\log \frac{n(\text{Ba})}{n(\text{He})}$	$\log \frac{n(\text{Ca})}{n(\text{He})}$	$\frac{\dot{M}_{\text{PB(S)}(\text{Sr})}}{\dot{M}_{\text{PB(S)}(\text{Ca})}}$	$\frac{\dot{M}_{\text{PB(S)}(\text{Ba})}}{\dot{M}_{\text{PB(S)}(\text{Ca})}}$
GD 362	< -10.7	-6.24	2.5e-4	< 2.9e-4
PG 1225–079	< -11.6	-8.06	< 8.8e-4	< 1.9e-3

**Notes.** We follow standard astronomical usage to report photospheric abundances by number, denoted by  $n$ . We follow standard cosmochemical usage and compare parent body mass ratios, denoted by  $\dot{M}$ .

abundances and inferred results for the relative mass accretion rates of Sr and Ca also are provided.

The more stringent result is found for GD 362. For this star, we find from Equation (8) that less than 0.4% of the accreted calcium is from material with the composition of Earth’s continental crust. Consequently, the crustal contribution to the contamination of GD 362 (Xu et al. 2013) is mostly basaltic; there is no evidence for any material produced by plate tectonics. For PG 1225–079, the corresponding result is that less than 20% of the calcium is derived from material compositionally similar to continental crust.

### 3.4. Strontium Limits

From Table 2, we find for GD 362 that the Sr/Ca abundance ratio is even less than in CI chondrites. This is not expected in our model and when more data become available, more sophisticated models can be developed. For PG 1225–079, there is no evidence that Sr is measurably enhanced beyond its relative concentration in CI meteorites.

## 4. DISCUSSION

At least in the solar system, the total mass in continental crust is greater than the mass in asteroids. Therefore, even though asteroids dominate the accretion onto white dwarfs, there might be favorable circumstances where the planetary contribution

to the heavy elements polluting a white dwarf’s photosphere is measurable. For example, at Earth, while most meteorites are derived from asteroids, about 0.07% originate in the crust of Mars.<sup>5</sup> Detailed simulations for a wide variety of orbital architectures are required to compare the rate of collisional erosion of a planetary crust with the rate of asteroid destruction and, for both processes, the subsequent accumulation onto the host white dwarf.

Consider a strategy to extend the pilot search reported here. In DZ stars, the equivalent width of Ca II 3933 Å can exceed 30 Å (Sion et al. 1990); these stars typically are identified with low-resolution spectra (Dufour et al. 2007; Koester et al. 2011). With follow-up high spectral resolution studies of members of this class of stars, it should be possible to make useful measures of the Sr and Ba abundances to compare with different crustal abundances.

## 5. CONCLUSIONS

Available data allow us to conclude that the abundances of Sr and Ba relative to Ca in two externally polluted white dwarfs are much less than found in Earth’s continental crust. Consequently, to date, there is no evidence for extrasolar Earth-analog plate tectonics. Given the intense theoretical interest in this topic, additional targets can and should be studied.

This work has been partly supported by the NSF. We thank D. Koester for computing the model atmospheres and elemental settling times employed here.

## REFERENCES

- Becklin, E. E., Farihi, J., Jura, M., et al. 2005, *ApJL*, 632, L119  
 Bercovici, D., & Yanick, R. 2013, *E&PSL*, 365, 275  
 Bond, J. C., O’Brien, D. P., & LaRetta, D. S. 2010, *ApJ*, 715, 1050  
 Debes, J. H., & Sigurdsson, S. 2002, *ApJ*, 572, 556

<sup>5</sup> <http://curator.jsc.nasa.gov/antmet/statistics.cfm>: as of 2012, 12 Martian meteorites have been detected out of a collection of 653 achondrites and 17,672 chondrites.

- Dufour, P., Bergeron, P., Liebert, J., et al. 2007, *ApJ*, **663**, 1291
- Farihi, J., Gaensicke, B. T., & Koester, D. 2013, *Sci*, **342**, 218
- Farihi, J., Jura, M., Lee, J.-E., & Zuckerman, B. 2010, *ApJ*, **714**, 1386
- Foley, B. J., Bercovici, D., & Landuyt, W. 2012, *E&PSL*, **331**, 281
- Gaensicke, B. T., Koester, D., Farihi, J., et al. 2012, *MNRAS*, **424**, 333
- Gladman, B. J., Burns, J. A., Duncan, M., Pascal, L., & Levison, H. F. 1996, *Sci*, **271**, 1387
- Jura, M. 2003, *ApJL*, **584**, L91
- Jura, M. 2008, *AJ*, **135**, 1785
- Jura, M., Farihi, J., Zuckerman, B., & Becklin, E. E. 2007, *AJ*, **133**, 1927
- Jura, M., & Xu, S. 2012, *AJ*, **143**, 6
- Jura, M., Xu, S., Klein, B., Koester, D., & Zuckerman, B. 2012, *ApJ*, **750**, 69
- Jura, M., Xu, S., & Young, E. D. 2013, *ApJL*, **775**, L41
- Jura, M., & Young, E. D. 2014, *AREPS*, **42**, 45
- Kilic, M., von Hippel, T., Leggett, S. K., & Winget, D. E. 2005, *ApJL*, **632**, L115
- Kite, E. S., Manga, M., & Gaidos, E. 2009, *ApJ*, **700**, 1732
- Klein, B., Jura, M., Koester, D., & Zuckerman, B. 2011, *ApJ*, **741**, 64
- Klein, B., Jura, M., Koester, D., Zuckerman, B., & Melis, C. 2010, *ApJ*, **709**, 950
- Koester, D. 2009, *A&A*, **498**, 517
- Koester, D. 2010, *MmSAI*, **81**, 921
- Koester, D., Girven, J., Gaensicke, B. T., & Dufour, P. 2011, *A&A*, **530**, 114
- Korenaga, J. 2010, *ApJL*, **725**, L43
- Korenaga, J. 2012, *NYASA*, **1260**, 87
- Lenardic, A., & Crowley, J. W. 2012, *ApJ*, **755**, 132
- Lodders, K. 2003, *ApJ*, **591**, 1220
- Mashonkina, L., Gehren, T., & Bikmaev, I. 1999, *A&A*, **343**, 519
- McSween, H. Y. 1985, *RvGeo*, **23**, 391
- Mittlefehldt, D. W. 2004, *TrGeo*, **1**, 291
- O'Neill, C., & Lenardic, A. 2007, *GeoRL*, **34**, L19204
- O'Rourke, J. G., & Korenaga, J. 2012, *Icar*, **221**, 1043
- Reddy, B. E., Tomkin, J., Lambert, D. L., & Prieto Allende, C. 2003, *MNRAS*, **340**, 304
- Rudnick, R. L., & Gao, S. 2003, *TrGeo*, **3**, 1
- Sion, E. M., Kenyon, S. J., & Aannestad, P. A. 1990, *ApJS*, **72**, 707
- Stamenkovic, V., Breuer, D., & Spohn, T. 2011, *Icar*, **216**, 572
- Stamenkovic, V., Noack, L., Breuer, D., & Spohn, T. 2012, *ApJ*, **748**, 41
- Stein, C. A., Lowman, J. P., & Hansen, U. 2013, *E&PSL*, **361**, 448
- Taylor, S. R., & McLennan, S. M. 2009, in *Planetary Crusts* (Cambridge: Cambridge Univ. Press)
- Treiman, A. H., Gleason, J. D., & Bogard, D. D. 2000, *P&SS*, **48**, 1213
- Valencia, D., & O'Connell, R. J. 2009, *E&PSL*, **286**, 492
- Valencia, D., O'Connell, R. J., & Sasselov, D. D. 2007, *ApJL*, **670**, L45
- van Heck, H. J., & Tackley, P. J. 2011, *E&PSL*, **310**, 252
- van Summeren, J., Conrad, C. P., & Gaidos, E. 2011, *ApJL*, **736**, L15
- Wasson, J. T., & Kallemeyn, G. W. 1988, *RSPTA*, **325**, 535
- Xu, S., Jura, M., Klein, B., Koester, D., & Zuckerman, B. 2013, *ApJ*, **766**, 132
- Xu, S., Jura, M., Koester, D., Klein, B., & Zuckerman, B. 2014, *ApJ*, **783**, 79
- Zuckerman, B., Koester, D., Dufour, P., et al. 2011, *ApJ*, **739**, 101
- Zuckerman, B., Koester, D., Melis, C., Hansen, B., & Jura, M. 2007, *ApJ*, **671**, 872